



Contents lists available at ScienceDirect

Spectrochimica Acta Part A: Molecular and Biomolecular Spectroscopy

journal homepage: www.elsevier.com/locate/saa

Study on the photochromism, photochromic fluorescence switch, fluorescent and colorimetric sensing for Cu²⁺ of naphthopyran-diaminomaleonitrile dyad and recognition Cu²⁺ in living cells

Heyang Zhang¹, Tianyuan Zhong¹, Nan Jiang, Zhuo Zhang, Xue Gong, Guang Wang*

Key Laboratory of Nanobiosensing and Nanobioanalysis at Universities of Jilin Province, Faculty of Chemistry, Northeast Normal University, Changchun 130024, PR China

ARTICLE INFO

Article history:

Received 10 December 2019

Received in revised form 21 February 2020

Accepted 22 February 2020

Available online 24 February 2020

Keywords:

Photochromism

Photochromic fluorescence switch

Fluorescent and colorimetric chemosensor

Copper ions

Naphthopyran

ABSTRACT

A well-designed naphthopyran-diaminomaleonitrile dyad (sensor **1**) has been synthesized successfully, its molecular structure was well characterized by NMR and mass spectrometry. Sensor **1** exhibits excellent photochromic and photochromic fluorescence switch performance with reversible color change and good fatigue resistance upon alternating ultraviolet irradiation and thermal bleaching. In addition, sensor **1** displayed excellent fluorescent and colorimetric sensing ability towards Cu²⁺ ions with high selectivity and sensitivity. The addition of 5.0 equiv. of Cu²⁺ ions into sensor **1** (1×10^{-5}) in CH₃CN solution significantly quenched the fluorescence of sensor **1** by 80.0%. Furthermore, the addition of Cu²⁺ ions also caused the complete disappearance of the absorbance band at 350–450 nm in absorbance spectra of sensor **1** and accompanied by the distinct color change from yellow to colorless. Job's plot, mass spectrometry, ¹H NMR titration and DFT calculations proved that sensing performance was attributed to the formation of 1:1 sensor **1**-Cu²⁺ complexes. Sensor **1** can monitor the existence of Cu²⁺ ions in living cells via the fluorescence images. Sensor **1** showed great potential applications as chemosensor and photochromic materials.

© 2020 Elsevier B.V. All rights reserved.

1. Introduction

Photochromic materials have potential applications in optical switches, optical storage, optoelectronic devices and ultraviolet protecting due to their reversible photo-induced molecular isomerization between two isomers whose absorption spectra are distinguishably different [1–3]. Naphthopyran with excellent photochromic performance such as the breadth of color generated, excellent thermal reversibility, absence of background color, easy control over fading kinetics, and good resistance to photochemical fatigue has been extensively studied in the field optical storage, controlled release materials, chemosensors and fluorescent switches [4–7]. So exploring the new molecular naphthopyran with multiple functions is significant.

In recent years, fluorescent and colorimetric chemosensors are becoming increasingly important in recognition and detection of metal ions due to their fast recognition process, in-situ detection, precise accurateness and low-cost [8–11]. All heavy metal ions play an important role in organisms, in which, Cu²⁺ ions perform a dual effect on physiology of human beings [12,13]. On the one hand, Cu²⁺ ion is essential trace metal ion to sustain normal human health, for examples, Cu²⁺ ions sever as a cofactor

for a wide variety of enzymes in all living organisms and in various redox processes and pigments [14,15]. On the other hand, excess existence of Cu²⁺ in living body can cause some serious diseases, such as prion disease, neurodegenerative diseases, irritation of nose and throat resulting in nausea, vomiting, and diarrhea others [16–18]. Therefore, it is necessary to monitor and detect copper ions in water and other environmental samples. Although the traditional detection methods for Cu²⁺ ions such as atomic absorption spectroscopy (AAS) [19], inductively coupled plasma atomic emission spectrometry (ICP-AES) [20] and electrochemical methods (EM) [21] display high sensitivity and accuracy, their analysis process requires sophisticated equipment, tedious sample preparation procedure and trained operators [22]. Due to the easy detection operation, up to now, a variety of fluorescent and colorimetric chemosensors of Cu²⁺ ions including small organic molecules, polymers, nanoparticles were explored [23–26]. Even so, there is a need to explore new high sensitive and selective fluorescence chemosensor for Cu²⁺ ions is still necessary.

Schiff base, condensation of reactive aldehydes and amines, is a family of important compounds with various potential applications. Some of Schiff base compounds were used as electron donor to coordinate with metal ions in fluorescent chemosensors [27,28]. Diaminomaleonitrile has special steric structure and containing four nitrogen atoms, our research work had proved that it can selectively coordinate with Cu²⁺ ion and further induce the obvious fluorescence change of the whole molecule [29].

* Corresponding author.

E-mail address: wangg923@nenu.edu.cn (G. Wang).¹ These authors contributed equally to this work.

In this paper, a new Schiff base composed of naphthopyran and diaminomaleonitrile has been developed (Scheme 1). The designed Schiff molecule not only displayed good photochromic performance and photochromic fluorescence switch but also presented fluorescent and colorimetric sensing ability for Cu^{2+} ions in CH_3CN solution with high selectivity and sensitivity.

2. Experimental

2.1. General methods

Diaminomaleonitrile and 1,1-diphenyl-2-propyn-1-ol was purchased from Sinopharm Chemical Reagent Co., Ltd. *p*-Toluenesulfonic acid (PTSA) was recrystallized from ethanol. Solvents were purified by normal procedures and handled under moisture free atmosphere. The other materials were commercial products and used without further purification. The salts used in stock solutions of metal ions are PbCl_2 , $\text{Zn}(\text{NO}_3)_2 \cdot 6\text{H}_2\text{O}$, $\text{Cd}(\text{NO}_3)_2 \cdot 4\text{H}_2\text{O}$, $\text{Cu}(\text{NO}_3)_2 \cdot 3\text{H}_2\text{O}$, $\text{Co}(\text{NO}_3)_2 \cdot 6\text{H}_2\text{O}$, SrSO_4 , HgCl_2 , $\text{Cr}(\text{NO}_3)_3 \cdot 9\text{H}_2\text{O}$, $\text{FeSO}_4 \cdot 7\text{H}_2\text{O}$, $\text{Ni}(\text{NO}_3)_2 \cdot 6\text{H}_2\text{O}$, AgNO_3 , GaCl_3 , $\text{BaCl}_2 \cdot 2\text{H}_2\text{O}$, $\text{Al}(\text{NO}_3)_3 \cdot 9\text{H}_2\text{O}$, $\text{MnCl}_2 \cdot 4\text{H}_2\text{O}$, $\text{InCl}_3 \cdot 4\text{H}_2\text{O}$. All the stock solutions of metal ion were prepared in water.

^1H and ^{13}C NMR spectra were recorded on a Varian Unity Inova Spectrometer at room temperature using *d*-chloroform and dimethylsulfoxide- d_6 as solvent. CE-MS spectra were obtained on CESI 8000 Plus-Triple TOF4600 mass spectrometer. UV-Vis absorption and fluorescence spectra were measured on Varian Cary 500 spectrophotometer and Cary Eclipse Fluorescence Spectrophotometer, respectively. The ultraviolet light source for irradiation was CHF-XM35 parallel light system (Beijing Changming Technology Co. Ltd) with a 500 W xenon lamp and monochromatic filter (360 nm). The irradiating light reached to the samples was parallel and its intensity was 1.2 mW/cm^2 .

2.2. Synthesis of sensor 1

2.2.1. Synthesis of 3,3-diphenyl-[3H]naphtho[2,1-b]pyran-8-aldehyde (compound a)

1,1-Diphenyl-2-propyn-1-ol (1.668 g, 8 mmol), 6-Hydroxy-2-naphthaldehyde (2.096 g, 12 mmol) and *p*-toluenesulfonic acid (PTSA) (0.1 equiv.) were added into 60 mL dry CH_2Cl_2 and stirred under nitrogen atmosphere at room temperature for 40 h. The reaction mixture was washed with water and dried with anhydrous sodium sulfate. The crude product was purified by column chromatography on silica gel (eluent: CH_2Cl_2 :petroleum ether = 1:2) to give white powder, 1.64 g, yield 56.3%. ^1H NMR (500 MHz, CDCl_3), δ : 10.05 (s, 1H), 8.16 (s, 1H), 8.01 (d, 1H, $J = 9.0$ Hz), 7.92–7.90 (m, 1H), 7.78 (d, 1H, $J = 8.5$ Hz), 7.47 (d, 4H, $J = 7.5$ Hz), 7.34–7.30 (m, 4H), 7.28–7.24 (m, 4H), 6.30 (d, 1H, $J = 10$ Hz).

2.2.2. Synthesis of sensor 1

A solution of diaminomaleonitrile (0.40 g, 3.2 mmol) in 20 mL methanol was added into the solution of 3,3-Diphenyl-[3H]naphtho[2,1-b]pyran-8-aldehyde (0.89 g, 2.5 mmol) in 30 mL methanol. The reaction mixture was refluxed for 24 h and then cooled to room temperature. After the solvent was evaporated under reduced pressure, the crude product was dissolved into 100 mL CH_2Cl_2 . The obtained organic solvent

was washed with water for three times and dried with anhydrous sodium sulfate. The product was purified by silica gel column chromatography using CH_2Cl_2 :petroleum = 7:1 as eluent to give faint yellow powder, 0.7 g, yield, 62.3%. M.p. 184–186 °C. ^1H NMR (DMSO, 500 MHz), δ 8.33 (d, $J = 7.6$ Hz, 2H), 8.27 (d, $J = 10.5$ Hz, 1H), 8.13 (d, $J = 8.9$ Hz, 1H), 7.96 (d, $J = 12.2$ Hz, 2H), 7.85 (d, $J = 8.8$ Hz, 1H), 7.54 (d, $J = 9.8$ Hz, 1H), 7.48 (d, $J = 7.3$ Hz, 4H), 7.35 (dd, $J = 16.1$, 8.5 Hz, 5H), 7.25 (t, $J = 7.3$ Hz, 2H), 6.63 (d, $J = 10.0$ Hz, 1H). ^{13}C NMR (151 MHz, CDCl_3) δ 159.01, 157.15, 155.28, 144.51, 133.23, 130.36, 128.23, 126.98, 124.20, 122.36, 119.45, 118.92, 114.31, 113.72, 112.36, 108.95. HRMS Calcd. for $\text{C}_{30}\text{H}_{20}\text{N}_4\text{O}$ [$\text{M} + \text{H}^+$]: 452.1637, Found: 453.1717.

3. Results and discussion

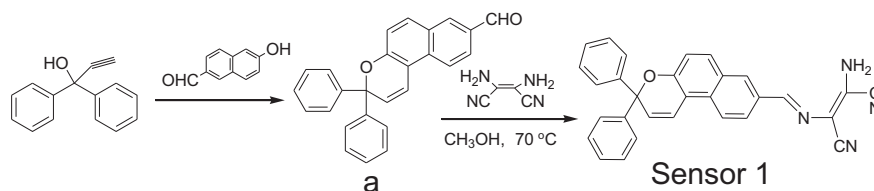
3.1. Design and synthesis of sensor 1

Our group has extensively studied on naphthopyran as photochromic materials in fluorescence switching and sensor, and also used diaminomaleonitrile as coordination unit to fabricate chemosensor for Cu^{2+} and Fe^{3+} ions [4–6,29]. In this paper, the naphthopyran and diaminomaleonitrile were combined by Schiff base to prepare a bifunctional compound (sensor 1) with photochromic properties and sensing ability. The molecular structure of sensor 1 was well characterized with ^1H NMR, ^{13}C NMR and mass spectroscopic methods (Figs. S1 and S2). It is interesting that sensor 1 not only displayed excellent photochromic property but also presented selective fluorescence and colorimetric sensing ability for Cu^{2+} ions.

3.2. Photochromic performance and photochromic fluorescence switch of sensor 1

3.2.1. Photochromic performance

The absorbance spectra of sensor 1 (1×10^{-5} M) in CH_3CN solution were shown in Fig. 1. The absorption band was at between 338–410 nm with two maximum absorption peak at 363 nm and 382 nm, which was ascribed to the π - π^* electron transition of naphthopyran [6,7]. After UV light irradiation, the new absorbance band between 405–600 nm with a peak at 487 nm appeared and gradually increased with the irradiation time indicating the occurrence of ring-open reaction of naphthopyran ring. The absorbance reached the maximum value after UV irradiation for 5 min accompanied by color change of the solution from colorless to light brown (insert in Fig. 1b). The naphthopyran unit on sensor 1 underwent an electrocyclic pyran-ring opening with cleavage of the C (sp^3)-O bond. The photochromic reaction of naphthopyran molecule is illustrated in Fig. 1a, the more planar structure (the so called 'open form' including TT and TC structures) with greater conjugation formed, which is responsible for the increased absorption band in the visible range of the spectrum. After ceasing of UV irradiation and the solution was put in the dark, the open-form of naphthopyran converted back to the closed-form accompanied by the gradually disappearing of the absorbance band in visible range and the color of solution via the thermal effect [30,31]. The absorption intensity at 487 nm gradually decreased with time and dropped down near to the original level after 1 h, the fading curve of the absorption intensity at 487 nm as the function of time was displayed in Fig. 1c. The fading kinetic was evaluated by



Scheme 1. The synthetic route of sensor 1.

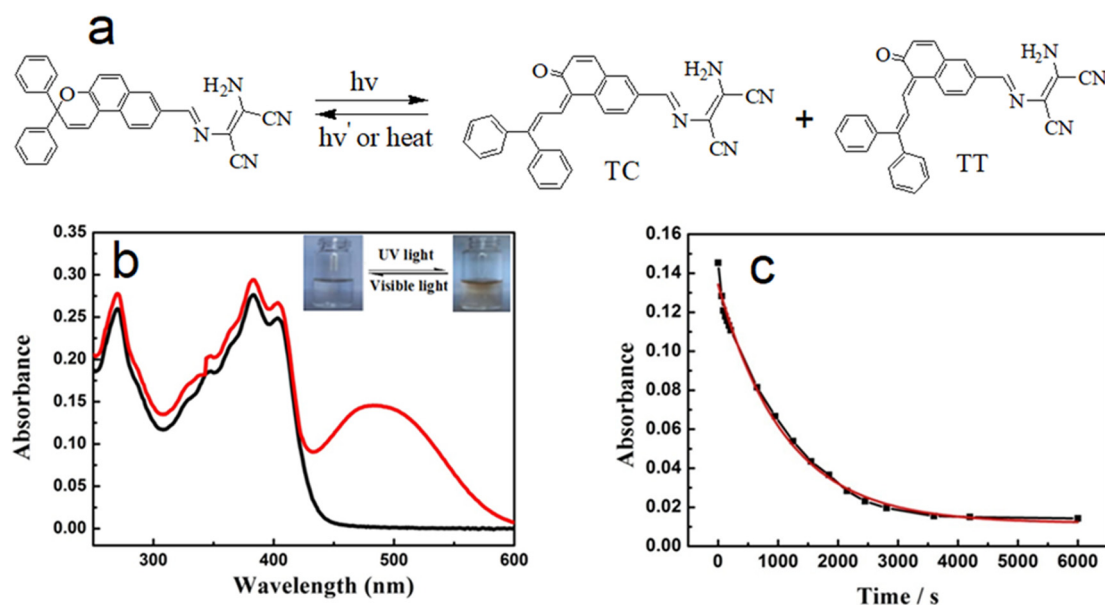


Fig. 1. a) The photochromic reaction of sensor **1**; b) the changes of the absorbance spectra and color of sensor **1** in (1×10^{-5} M) in CH_3CN solution before (black) and after (red) UV light irradiation; c) the kinetic curve of sensor **1** in (1×10^{-5} M) in CH_3CN solution monitored at 487 nm. (For interpretation of the references to color in this figure legend, the reader is referred to the web version of this article.)

fitting the following biexponential equation [32]: $A(t) = A_1 e^{-k_1 t} + A_2 e^{-k_2 t} + A_{th}$ with the experimental data. The fitting curve derived from Origin 8.0 computer program was almost superimposed over the experimental plot and the correlation coefficient of the curve fitting (R) was greater than 0.999, which indicated that biexponential model is suitable for photo-kinetic analysis of sensor **1**. All the fading kinetic constants were shown in Table 1. The fading speed was slower and the half-life period 600 s was obvious longer than those in other reports [4,31,33], which may be due to the formation of large conjugation with diaminomaleonitrile moiety via Schiff base unit.

The fatigue resistance is an important parameter for practical application. Upon the alternative UV irradiation for 5 min and putting in the dark for 1 h, the colorless solution of sensor **1** in CH_3CN changed alternately between colorless and orange. In the meantime, the absorption band of open-form naphthopyran centered at 487 nm rose and decayed alternately, which indicated that the ring-open and ring-close reactions alternately proceeded upon the alternative UV irradiation and putting in the dark. The reproducibility of absorbance at 487 nm after each coloration/fading sequence was shown in Fig. 2a and no marked absorption degradation was observed after 6 cycles (Fig. 2b). All above results demonstrated that sensor **1** had an excellent photochromic performance and great potential application value as a photochromic candidate.

3.2.2. Photochromic fluorescence switch

The sensor **1** also displayed strong fluorescence emission (Fig. 3a) and emission band was between 417 and 680 nm with maximum emission peak at 520 nm ($\lambda_{ex} = 385$ nm). Our previous research results demonstrated naphthopyran unit only emitted very weak fluorescence, and diaminomaleonitrile almost had no fluorescence emission, therefore the fluorescence emission of sensor **1** came from the conjugation system of whole molecule of sensor **1**. Naphthopyran moiety has been used to fabricate the photochromic fluorescence switches via the energy transfer mechanism [5,6,34], therefore the modulation effect of

isomerization of naphthopyran on the fluorescence of sensor **1** was also investigated. Fig. 1 demonstrated that UV irradiation induced the ring-open reaction of naphthopyran accompanied by the appearance of the new absorbance band. The new absorbance band overlapped with the fluorescence band at a large extent, it is reasonable to speculate that the energy transfer could take place and the fluorescence of sensor **1** will be quenched. However, it was unexpected that the fluorescence of sensor **1** (1×10^{-5} M) in CH_3CN solution after UV light irradiation was not quenched but enhanced gradually upon the UV irradiation time, as shown in Fig. 3a. The fluorescence intensity at 520 nm was enhanced by 19.6% $[(I-I_0)/I_0]$ after UV irradiation for 15 min, and would not further increase if the irradiation time was increased. This result illustrated the fluorescence emission of sensor **1** can't be absorbed by the open-ring form of naphthopyran. The fluorescence of sensor **1** came from its whole molecule, so it is reasonable to deduce that the fluorescence enhancement was caused by the enlarged conjugation system of the whole molecule due to the planar structure of open-ring naphthopyran. After UV irradiation, the solution was put in the dark for 1 h, the fluorescence band decreased to the original location before UV irradiation, which was due to the ring-close isomerization of pyran ring. This result demonstrated that sensor **1** had the property of the fluorescence switch and the fluorescence intensity could be modulated in the range of 0–19.6%. The fatigue resistance is an important factor for a fluorescence switch, so the fluorescence intensity at 520 nm was measured upon the alternative UV irradiation for 15 min and put in the dark for 1 h, the result was shown in the Fig. 3b. The reproducibility can be seen after each UV irradiation/put in the dark sequence and the fluorescence degradation was not observed after 6 cycles. All the above result demonstrated that sensor **1** possessed the excellent photochromic fluorescence switch performance. In addition, this result also illustrated that the fluorescence emission can't be absorbed by its open-ring structure.

3.3. Fluorescent sensing of sensor 1 towards Cu^{2+} ion and fluorescence images of live cells

3.3.1. Fluorescent sensing of sensor 1 towards Cu^{2+} ions

Diaminomaleonitrile can selectively coordinated with metal ions and further influence the photophysical properties of the whole compound in which it existed [29,35]. Therefore, the effect of metal ions on the photophysical properties was investigated.

Table 1

Kinetic data of sensor **1** in CH_3CN solution.

λ_{max} (nm)	A_1	A_2	A_{th}	$k_1 \times 10^{-2}$ (s^{-1})	$k_2 \times 10^{-2}$ (s^{-1})	$t_{1/2}$ (s)	R
487	0.0214	0.1237	0.00786	14.09	6.9	600	0.9997

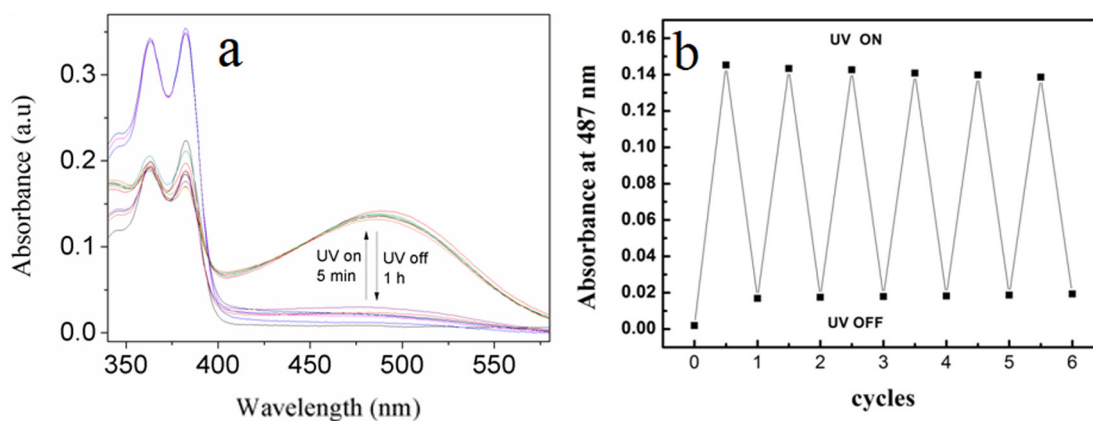


Fig. 2. a) The changes of the absorbance spectra of sensor **1** (1×10^{-5} M) in CH_3CN solution upon the UV irradiation and thermal fading at room temperature. b) the photochromic cycles of sensor **1** (1×10^{-5} M) in CH_3CN solution monitored at 487 nm before and after sequential steps of UV irradiation and being put in the dark. (For interpretation of the reference to color in this figure, the reader is referred to the web version of this article.)

The first factor to consider for a chemosensor is high selectivity. Many factors, such as the polarity, solubility, pH value and protophilia affected the selectivity of sensor. Therefore, the pure solvents DMSO, CH_3CN and THF, the mixed solvents containing Tris buffer (10 mM, pH = 7.2), DMSO:H₂O (1:1, V:V), THF:H₂O (1:1, V:V), THF:H₂O (4:1, V:V) and CH_3CN :H₂O (1:1, V:V) were used to investigate the absorbance and fluorescence responses of sensor **1** to metal ions. In the most above solvent systems, sensor **1** displayed irregular response to different metal ions. Only in pure CH_3CN , sensor **1** showed satisfactory high selective absorbance and fluorescence response towards Cu^{2+} ions.

Sensor **1** in this work displayed high fluorescent emission capacity, so we try to explore its availability as a sensitive and selective fluorescence chemosensor. Fig. 4a showed the fluorescence spectra of sensor **1** (1×10^{-5} M) in CH_3CN solution and its mixed solution with different metal ions (5 equiv. of sensor **1**). Sensor **1** itself in CH_3CN solution emitted strong fluorescence with an emission peak at 520 nm under the excitation of UV light of 385 nm. Naphthopyran is less fluorescence and diaminomaleonitrile itself hardly emits fluorescence, so it is reasonable to speculate that the fluorescence of sensor **1** originated from the whole molecule of sensor **1**. Expect for Cu^{2+} ion, the addition of the following metal ions including Zn^{2+} , Cd^{2+} , Hg^{2+} , Co^{2+} , Al^{3+} , Cr^{3+} , In^{3+} , Pb^{2+} , Sr^{2+} , Ag^{+} , Ni^{2+} , Ca^{3+} , Fe^{2+} , Mn^{2+} and Ba^{2+} ions did not give obvious effect on the fluorescence spectra of sensor **1** and just caused a small fluctuation up and down. On the contrary, the addition of 5 equiv. Cu^{2+} ions caused the remarkable fluorescence quenching by 80.0% calculated from the fluorescence intensity at 520 nm and the fluorescence changed from “on” to “off”. The fluorescence photographs of the above solutions further illustrated the selective quenching effect of Cu^{2+} ion on the

fluorescence of sensor **1**. Under the irradiation of 360 nm light, the sensor **1** solution displayed bright yellow fluorescence, the addition of the abovementioned metal ions did not cause the obvious fluorescence changes, as shown in Fig. 4b. The yellow fluorescence of the solution with Cu^{2+} ions only disappeared completely indicating the strong fluorescence quenching effect of Cu^{2+} ion on the sensor **1**. These results indicated that sensor **1** had the high selective fluorescence response towards Cu^{2+} ions. Therefore, based on the changes of fluorescence spectra and fluorescence color, it is safe to say that sensor **1** could be used as a selective fluorescent sensor to recognize and monitor the existence of Cu^{2+} ions.

The fluorescence quenching of sensor **1** by Cu^{2+} ion can be ascribed to its coordination with Cu^{2+} ion. Cu^{2+} ion and sensor **1** are tightly combined after complexation, the ligand to metal charge transfer (LMCT) from the excited states of sensor **1** to the d-orbitals of copper ions in the complex molecule occurred due to the strong paramagnetic nature of Cu^{2+} ion, which thus quenched the fluorescence. The other competitive metal ions did not form stable complexes and just cause the negligible fluorescence change, which may be due to the following two reasons. One was the unsuitable spatial coordination geometry conformation of diaminomaleonitrile, another was the inappropriate ion radius and insufficient binding energy of these metal ions for ligand. This kind of the fluorescence quenching mechanism of chemosensors by Cu^{2+} ion have been explained in previous reports [36,37].

The stoichiometry of sensor **1**- Cu^{2+} complex was tested by Job's plot method, a constant total concentration (2×10^{-5} M) of sensor **1** and Cu^{2+} and their molar ratio varied. And then, the fluorescence spectra of solutions were measured and the emission intensity at 520 nm was

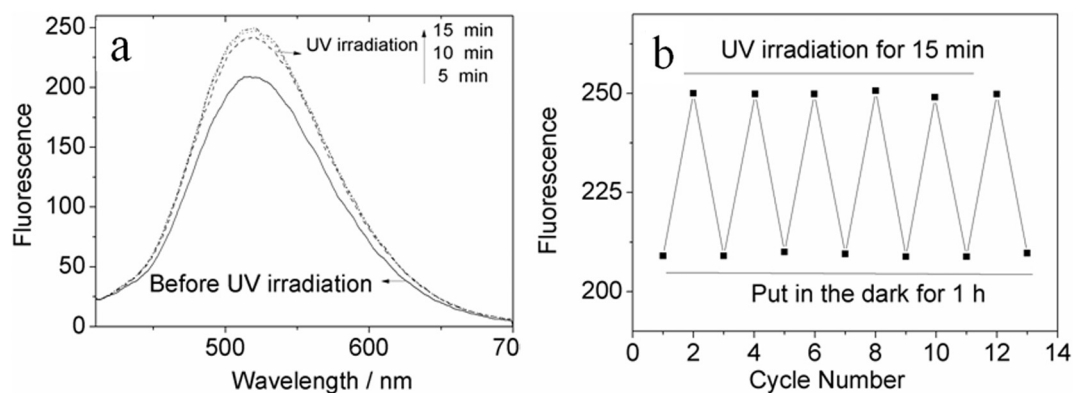


Fig. 3. a) The changes of the fluorescence spectra of sensor **1** (1×10^{-5} M) in CH_3CN solution after UV irradiation. b) The fluorescence fatigue resistance upon the alternative UV irradiation for 15 min and put in the dark for 1 h.

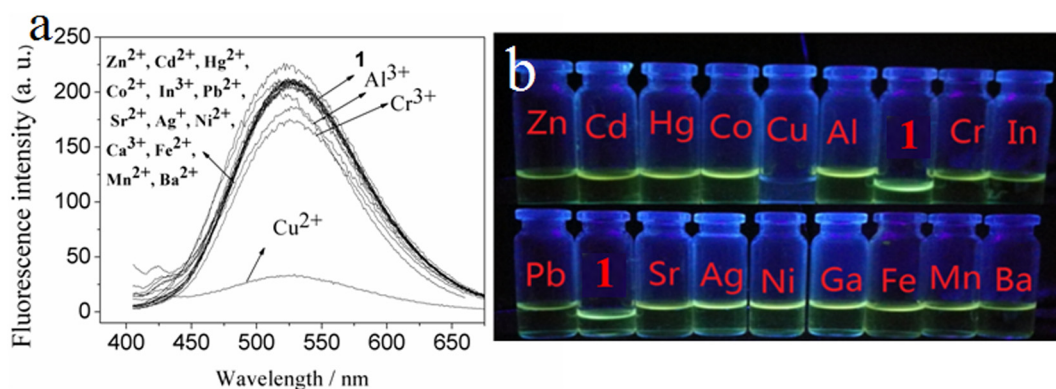


Fig. 4. Fluorescence spectra (a) and fluorescence photographs (b) of sensor **1** (1×10^{-5} M) in CH_3CN solution and its mixed solution with different metal ions (5 equiv. of sensor **1**, respectively).

plotted against the fraction of Cu^{2+} ions and the maximum value appeared at very close to 0.5 M fraction on the Job's plot pointing out 1:1 binding stoichiometry between sensor **1** and Cu^{2+} ion (Fig. 5a). The stoichiometry was then confirmed by positive ESI-HRMS. After adding the excess Cu^{2+} salt into the sensor **1** solution in DMSO and shaking for enough time to finish the complexing reaction, the supernatant was taken out to be measured for MS spectrum (Fig. S4). The mass spectrum of [sensor **1** + Cu^{2+}] showed a peak at $m/z = 515.0439$, which was attributed to [sensor **1** + Cu^{2+} - H^+] $^+$ (calcd. 514.0855). These results confirmed the formation of sensor **1**- Cu^{2+} complex with 1:1 stoichiometry.

Another necessary consideration is the anti-interference ability of sensor **1** towards the competitive metal ions. The competitive experiments could further confirmed the selectivity of sensor **1** to Cu^{2+} and evaluate the interference effect of the coexistence metal ions on the detection of sensor **1** for Cu^{2+} ions. Therefore, the competitive experiment was carried out by measuring the fluorescence intensity at 520 nm of the series of the solutions of sensor **1** in CH_3CN (1×10^{-5} M) containing 5 equiv. of Cu^{2+} ion and 20 equiv. of the other metal ions. From the result as shown in Fig. 5b, all the fluorescence under the coexistence of Cu^{2+} ion and any one of the above test metal ions was quenched to the similar level of that only existence of Cu^{2+} ion. This result demonstrated that the coexistence of other metal ions did not interfere with fluorescent sensing of sensor **1** for Cu^{2+} ion and further indicated sensor **1** possessed the practical application potential of sensing Cu^{2+} ions.

The fast fluorescence response of sensor **1** towards Cu^{2+} ion was more favorable for the real-time detection. After the addition of 5

equiv. of Cu^{2+} ion into the sensor **1** (1.0×10^{-5} M) in CH_3CN solution, the fluorescence intensity at 520 nm was monitored, the result was shown in Fig. S5. The fluorescence intensity gradually decreased with time and reached the lowest level after 15 min, which indicated sensor **1** had a fast fluorescence response towards Cu^{2+} ion and was suitable in the real-time test.

The fluorescence titration was also used to investigate the sensing properties. Here, the fluorescence titration experiment of sensor **1** (1×10^{-5} M) in CH_3CN solution upon the incremental addition of Cu^{2+} ion from 0.5–5 equiv. The fluorescence spectra gradually decreased with the increase of Cu^{2+} ion (Fig. 6a) and the fluorescence intensity at 520 nm presented a very good linear relationship with the concentration of Cu^{2+} ions in the range of 0.01–0.1 mM with a correlation coefficient of $R^2 = 0.9813$ (Fig. 6b). The wide linear range is beneficial for practical quantitative measurements. The limit of detection (LOD) was also calculated to be $4.03 \mu\text{M}$ by the equation of $\text{LOD} = 3\sigma/k$, here k and σ were the slope of the calibration curve and standard deviation of the blank solutions, respectively. The obtained limit of detection was much lower than the limit of copper ($\sim 20 \mu\text{M}$) in drinking water permitted by US Environment Agency (EPA) [38] and general concentration of blood copper in normal individuals (1.57×10^{-5} – 2.36×10^{-5} M) defined by the U.S. Environmental Protection Agency [39]. This result indicated that sensor **1** possessed the practical sensing ability of quantitative detection of Cu^{2+} concentration in solution.

The affinity of sensor **1** with Cu^{2+} ion can be estimated using the data from fluorescence titration experiment. The association constant (K_a) for the sensor **1**- Cu^{2+} complex was evaluated using the Benesi-

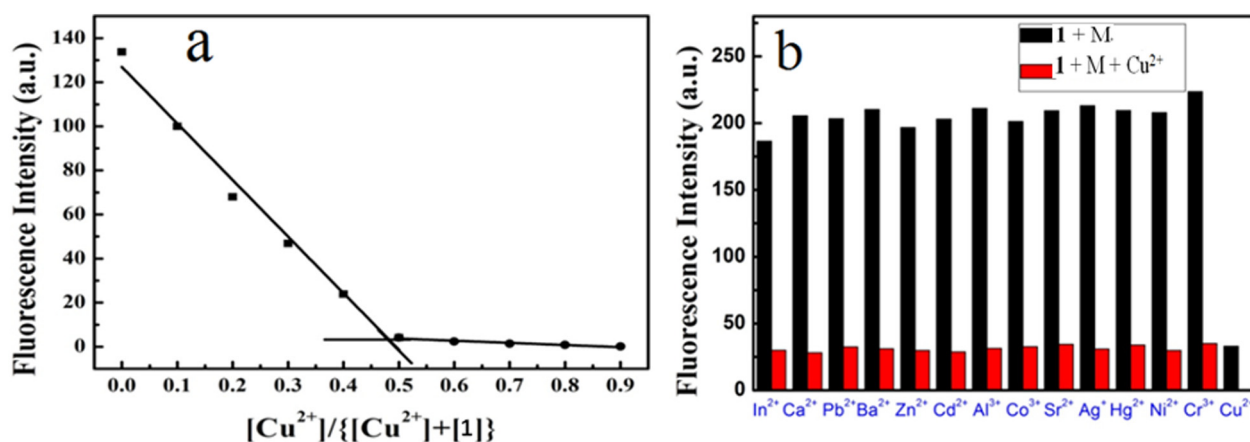


Fig. 5. a) Job's plot from the fluorescence intensity at 520 nm of sensor **1** and Cu^{2+} ion in CH_3CN solution with the total concentration of $20 \mu\text{M}$. b) Selectivity of sensor **1** (1×10^{-5} M) in CH_3CN solution with 5 equiv. of Cu^{2+} ions over other competitive metal ions (20 equiv. of sensor **1**).

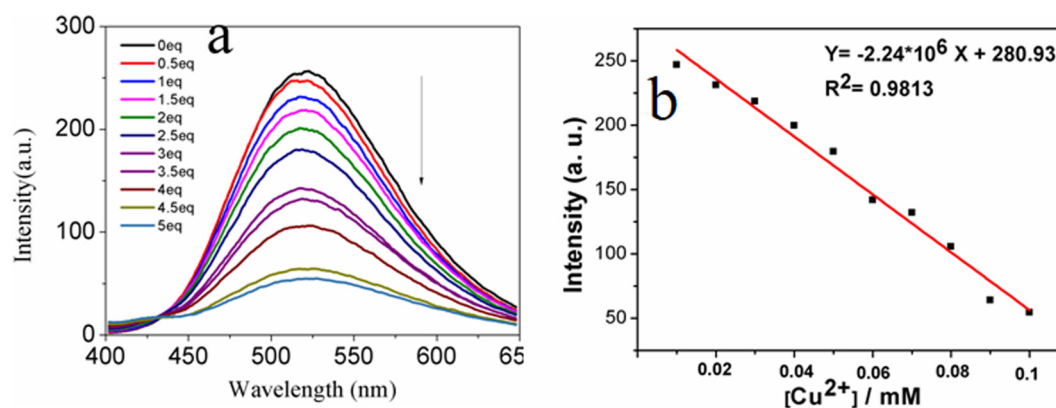


Fig. 6. a) The changes of fluorescence spectra of sensor **1** in CH_3CN solution (1×10^{-5} M) upon successive addition of Cu^{2+} (0.5–5 equiv.). (b) The changes of the fluorescence intensity at 520 nm of sensor **1** with the increase of Cu^{2+} concentration ($R^2 = 0.9813$).

Hildebrand (B-H) plot according to the following equation [30].

$$1/(F_0 - F) = 1/\{K_a(F_0 - F_{\min})C\} + 1/(F_0 - F_{\min})$$

where F_0 and F are the fluorescence intensities of sensor **1** only and in the presence of Cu^{2+} ions, C is the concentration of Cu^{2+} in the solution. F_{\min} is the minimum fluorescent intensity at 520 nm in the presence of excess Cu^{2+} ions. The fitted curve based on the 1:1 binding stoichiometry of sensor **1** and Cu^{2+} was linear and almost superimposed over the experimental plot with a correlation coefficient over 0.9881 (Fig. 7a), which further confirmed the 1:1 binding stoichiometry of sensor **1** with Cu^{2+} . K_a was calculated from the slope and intercept of the linear plot to be 8287 M^{-1} . The above results indicated that sensor **1** was a good candidate as a selective “on-off” fluorescent chemosensor for Cu^{2+} ions.

3.3.2. Stern-Volmer analysis

Stern-Volmer analysis was often used to confirm the fluorescence quenching nature of a fluorophore in the complexation process with metal ions. The plots of the fluorescence intensity (F_0/F or $\ln F_0/F$) at 520 nm of sensor **1** against the concentration of Cu^{2+} ion and showed a linear graph [34].

$$\frac{F_0}{F} = 1 + K_{SV}[M] \text{ dynamic quenching}$$

$$\ln \frac{F_0}{F} = e^{K_{SV}}[M] \text{ static quenching}$$

F_0 and F are the fluorescence intensities of sensor **1** at 520 nm in the absence and presence of Cu^{2+} ions, respectively. K_{SV} is the Stern-Volmer quenching constant and $[M]$ is the concentration of Cu^{2+} ion. As shown in Fig. 7b, within the range of test concentration, F_0/F (blue line) was not linear with Cu^{2+} concentration, which indicated the fluorescence quenching of sensor **1** upon the coordination by Cu^{2+} ions did not conform to dynamic quenching process. On the contrary, the $\ln F_0/F$ values displayed approximate linear relationship with Cu^{2+} concentration, the fitting linear relationship R^2 was 0.9507. This result was in agreement with the Perrin model of static quenching (black line), which further supports that fluorescence quenching in this systems occurs intramolecularly and also indicate that all the added Cu^{2+} ions were bound to sensor **1**.

3.3.3. Fluorescence imaging for live cells

In view of the fluorescence sensing performance of sensor **1** to Cu^{2+} ions, we investigated its practical application to monitor copper ion in living cells. The fluorescent cell imaging experiments were conducted using liver cancer HepG2 cells. First, the solutions of sensor **1** (1×10^{-5} M) in DMSO and Cu^{2+} ions (1×10^{-4} M) in the empty medium solution were prepared. Then, in each of well 1 and 2, 500 μL of cell suspension and 10 μL of Cu^{2+} solution were added. And after, the cells were incubated for 30 min at 37 $^\circ\text{C}$ and then washed three times with PBS. At last, well 1 was added 10 μL solution of sensor **1** and was further incubated for 50 min at 37 $^\circ\text{C}$ and washed three times with PBS. Finally, the cells were washed for three times with PBS solution and then were fixed, stained and mounted onto glass slides and the fluorescence images were taken under the excitation wavelength at

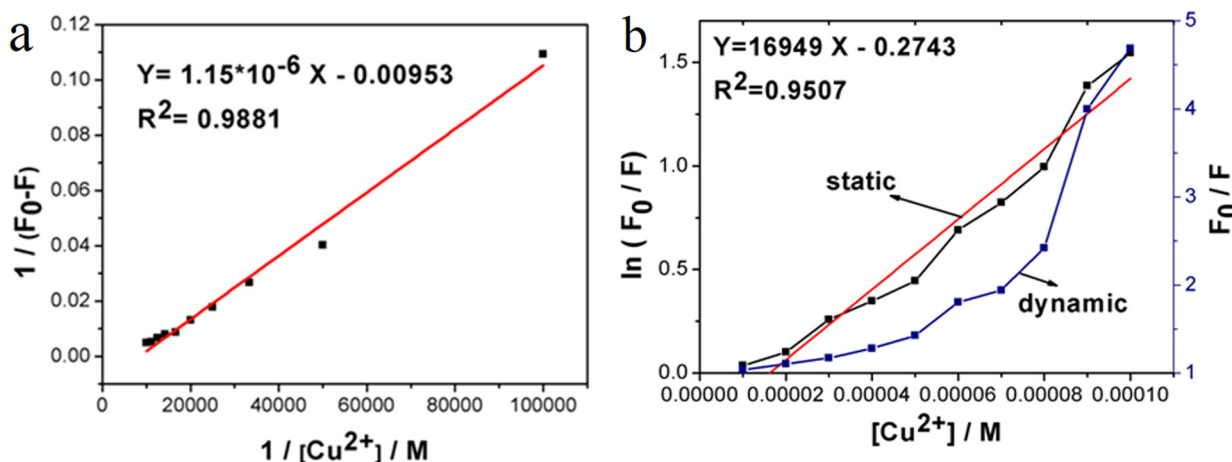


Fig. 7. a) Benesi-Hildebrand plot of sensor **1** upon gradual addition of Cu^{2+} ions. b) Stern-Volmer quenching plots for dynamic quenching and static quenching of sensor **1** by Cu^{2+} ion.

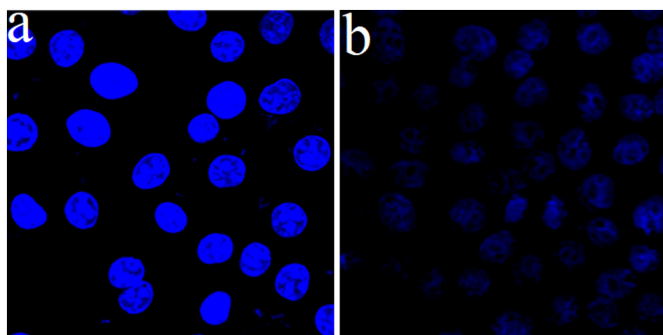


Fig. 8. Confocal fluorescence images of HepG2 cells. (a) fluorescence image of HepG2 cells pretreated just with sensor **1**. (b) fluorescence image of HepG2 cells pretreated with Cu^{2+} (1×10^{-4} M) for 30 min and then incubated with sensor **1** (1×10^{-5} M).

405 nm. The fluorescence images were shown in Fig. 8, the cells just treated only with sensor **1** showed bright blue fluorescence. Whereas, the fluorescence of the cells incubated with Cu^{2+} and sensor **1** almost disappeared, the residual blue color was the result of cell stain. These results indicated that sensor **1** can permeate the cell and coordinated with Cu^{2+} ions, which was accompanied by the fluorescence quenching. Based on these fluorescence images, it is safe to say that sensor **1** can be used to monitor the existence of Cu^{2+} ions in living cells.

3.4. Selective colorimetric sensing of sensor **1** towards Cu^{2+} ions

Previous studies on fluorescence spectra showed that sensor **1** could selectively coordinated with Cu^{2+} ions and further influenced the fluorescence properties of sensor **1**. Therefore, the changes of absorbance spectra and color of sensor **1** in CH_3CN solution upon the addition of Cu^{2+} ions was also investigated.

The most direct proof for selective colorimetric sensing ability of sensor **1** towards Cu^{2+} ion was that the yellow color of solution (3×10^{-5} M) in CH_3CN straightway turned to colorless after addition of Cu^{2+} ion (5.0 equiv. of sensor **1**) (Fig. 9a). On the contrary, the addition of the other metal ions including Zn^{2+} , Cd^{2+} , Hg^{2+} , Co^{2+} , Cu^{2+} , Al^{3+} , Cr^{3+} , In^{3+} , Pb^{2+} , Sr^{2+} , Ag^{+} , Ni^{2+} , Ga^{3+} , Fe^{2+} , Mn^{2+} and Ba^{2+} ions (5.0 equiv. of sensor **1**) did not induce the solution color change. This result directly indicated that the sensor **1** can selectively recognize Cu^{2+} ions and visually confirm the existence of Cu^{2+} ions.

The selective color change of sensor **1** solution upon the addition of Cu^{2+} ions was further confirmed by the absorbance spectra, shown in Fig. 9b. The addition of 5 equiv. Cu^{2+} ions reduced the absorbance band in wavelength range of 350 nm–450 nm nearly to vanished. Similar with the color change, the addition of the other metal ions did not cause the obvious changes, which further indicated the high selectivity and colorimetric sensing ability of sensor **1** towards Cu^{2+} ions.

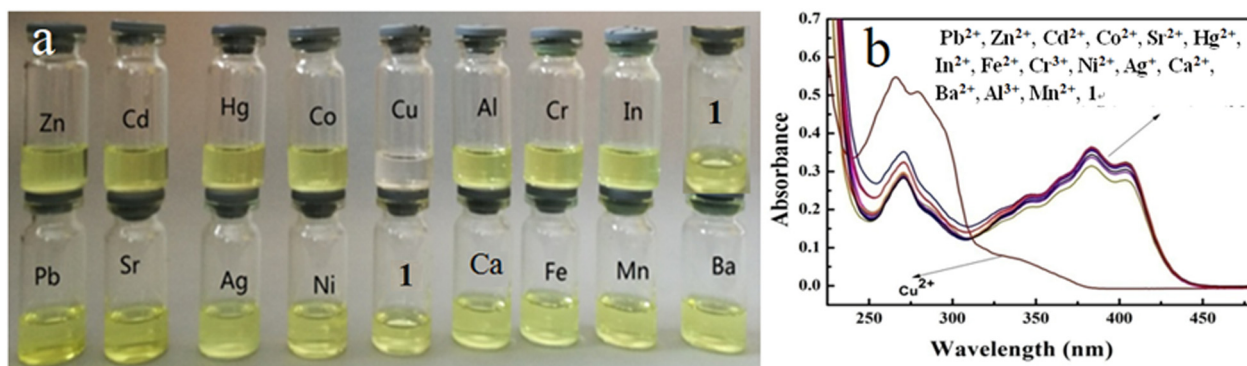


Fig. 9. a) The photographs of sensor **1** (3×10^{-5} M) in CH_3CN solutions containing different metal ions (5 equiv. of sensor **1**). (b) The absorbance spectra of sensor **1** (1×10^{-5} M) in CH_3CN solution and different metal ions (5 equiv. of sensor **1**). (For interpretation of the reference to color in this figure, the reader is referred to the web version of this article.)

The above obvious color change and absorption decrease of sensor **1** solution upon the addition of Cu^{2+} ions were also ascribed to the complexation between the electron-donating diaminomaleonitrile and acceptor Cu^{2+} ion. The other competitive metal ions did not form stable complexes and not cause the negligible change of the absorption spectra.

The next necessary consideration is anti-interference ability of sensor **1** towards the competitive metal ions. The competitive experiments could further confirmed the high selectivity of sensor **1** to Cu^{2+} ions. Therefore, the competitive experiment was carried out by measuring the absorbance spectra of the series of sensor **1** (1×10^{-5} M) in CH_3CN solutions containing 5 equiv. of Cu^{2+} ion and 5 equiv. of the other metal ions, respectively. As shown in Fig. 10a, the ordinate values are the absorbance at 382 nm, the absorption intensity of sensor **1**- Cu^{2+} at 382 nm in the presence of the other competitive metal ions was not influenced by the competitive metal ions. This result indicated that sensor **1** possessed the high colorimetric selectivity for Cu^{2+} ion and the other coexistent competitive cations did not interfere in the colorimetric sensing of sensor **1** for Cu^{2+} ion.

The UV–visible absorbance titration of sensor **1** by Cu^{2+} ions was also carried out in CH_3CN (1×10^{-5} M) to evaluate the colorimetric sensing sensitivity. The absorbance spectra of sensor **1** solution after addition of the different concentration of Cu^{2+} ions were recorded and shown in Fig. S6. The UV–vis absorption band at 330–450 nm decreased gradually with the increasing of Cu^{2+} ion. The absorption intensity at 382 nm showed good linear relationship with the Cu^{2+} concentration from 0 to 5 equiv. of sensor **1** with a correlation coefficient of $R^2 = 0.98951$ (Fig. S7). The better linear was in favor of quantitative detection of Cu^{2+} ions. In addition, the detection limit (LOD) was also calculated to be 5.39×10^{-4} mol/L from the calibration curve according to the equations $\text{LOD} = 3\sigma/K$ defined by IUPAC. Here, σ is the standard deviation of the blank measurement and K is the slope of the calibration curve of the absorption intensity as a function of Cu^{2+} concentration [32,33].

The associate constants (K_a) for the interaction of sensor **1** with Cu^{2+} ion was also estimated from the titration data using the Benesi–Hildebrand plot according to the following equation [10].

$$\frac{1}{A_0} - A = \frac{1}{K_a} \times (A_0 - A_{min}) \times C + \frac{1}{A_0} A_{min}$$

where A and A_0 are the absorption intensities at 382 nm in the present of any given concentration and in the absence of Cu^{2+} ion, respectively. A_{min} is the lowest value of the absorption intensity at 382 nm in the presence of excess Cu^{2+} ions. The Benesi–Hildebrand plot was drawn using $1/(A_0 - A)$ as function of $1/[\text{Cu}^{2+}]$ and showed a linear plot (Fig. 10b). The fitting plot based on 1:1 stoichiometry (sensor **1**: Cu^{2+}) is almost superimposed over the experimental curve with a correlation coefficient over 0.99934 indicating the 1:1 binding mode of sensor **1**- Cu^{2+} complex. The associate constant K_a of sensor **1** with Cu^{2+} was

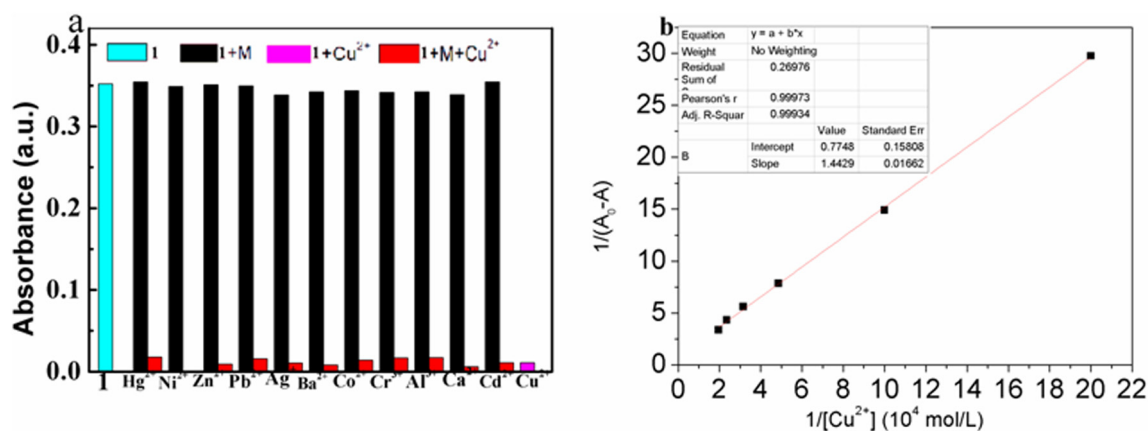


Fig. 10. a) Absorbance response at 382 nm of sensor **1** (1×10^{-5} M) in CH_3CN solution upon the addition of different metal ions (5.0 equiv. of sensor **1**). b) Benesi-Hildebrand plot of sensor **1** in CH_3CN solution (1×10^{-5} M) in the presence of Cu^{2+} ($0\text{--}5 \times 10^{-5}$ M) ($R^2 = 0.99934$). (For interpretation of the reference to color in this figure, the reader is referred to the web version of this article.)

calculated from the slope and the intercept of the fitting line to be 5370 M^{-1} , this value was close to K_a obtained from fluorescence titration. The large affinity also verified sensor **1** was sensitive enough to sense Cu^{2+} ions in solution over the other metal ions. Although the sensing performance of sensor **1** was carried out in non-aqueous solvent, the metal ions were in pure water solutions. Therefore, sensor **1** could be useful for the detection of Cu^{2+} ions in chemical and environmental samples.

3.5. Proposed binding mode

The above results of Job's plot, mass spectra and Benesi-Hildebrand plot had confirmed the 1:1 complexing mode of sensor **1** with Cu^{2+} ion. To further study the binding mode of sensor **1** with Cu^{2+} ions in greater detail, ^1H NMR titrations of sensor **1** by Cu^{2+} ion in $\text{DMSO}-d_6$ and the theoretical calculations were conducted to interpret and ascertain the complex mode of sensor **1** with Cu^{2+} ion.

The ^1H NMR spectral changes of sensor **1** upon the incremental addition of Cu^{2+} ions were shown in Fig. S8. The proton singlets of

naphthalene on sensor **1** showed slight downshift and widening with the gradual addition of Cu^{2+} ions, which was ascribed to the coordination of diaminomaleonitrile moiety with Cu^{2+} ion. The result of ^1H NMR indicated the existence of interaction of sensor **1** with Cu^{2+} ion.

To further clarify the coordination mode of sensor **1** with Cu^{2+} ions, density functional theory (DFT) calculations with the Gaussian 09 program were carried out to provide a theoretical explanation [40]. The CYL view program was used to generate the 3D molecular structures [41]. All studied complexes were optimized at the B3LYP level [42] of density functional theory, together with vibrational frequency calculations to obtain minima of energy. The LANL2DZ was employed for the Cu atom with effective core potentials (ECPs) for its core electrons [43,44]. The 6-31G(d) basis set was used to describe the C, H, O and N atoms [45].

As shown in Fig. 11, the optimized molecular modeling structures of sensor **1** and sensor **1**- Cu^{2+} ion disclosed the 1:1 stoichiometry of sensor **1**- Cu^{2+} complex via the coordination of nitrogen atoms of cyan with copper atom. On the free sensor **1**, the highest occupied orbit (HOMO) was mainly distributed on naphthalene unit and benzene ring. Different

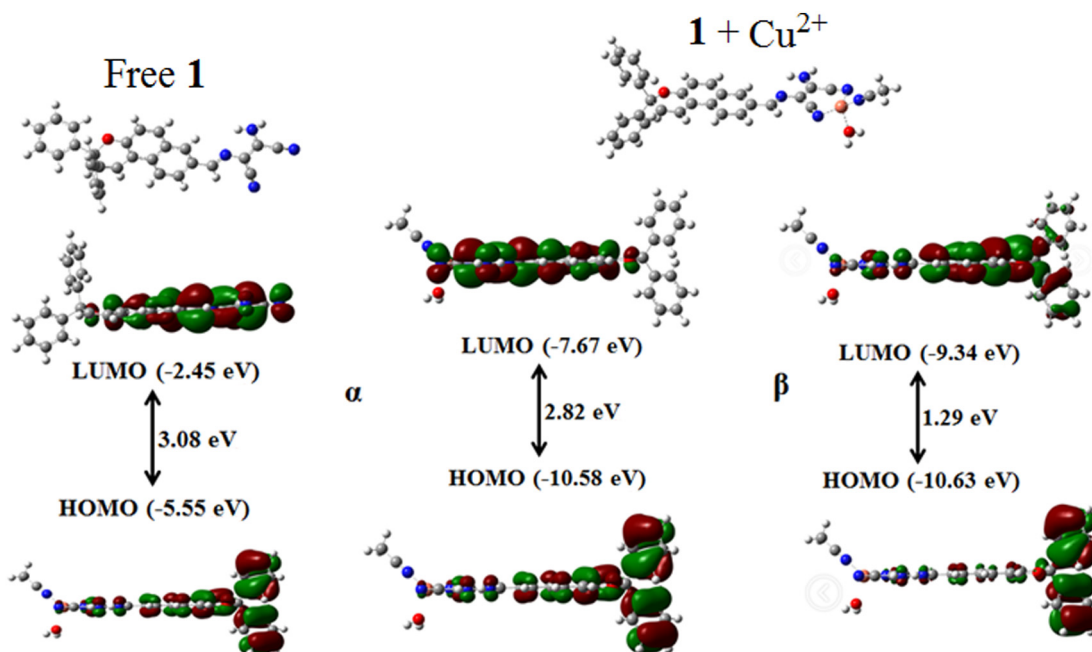
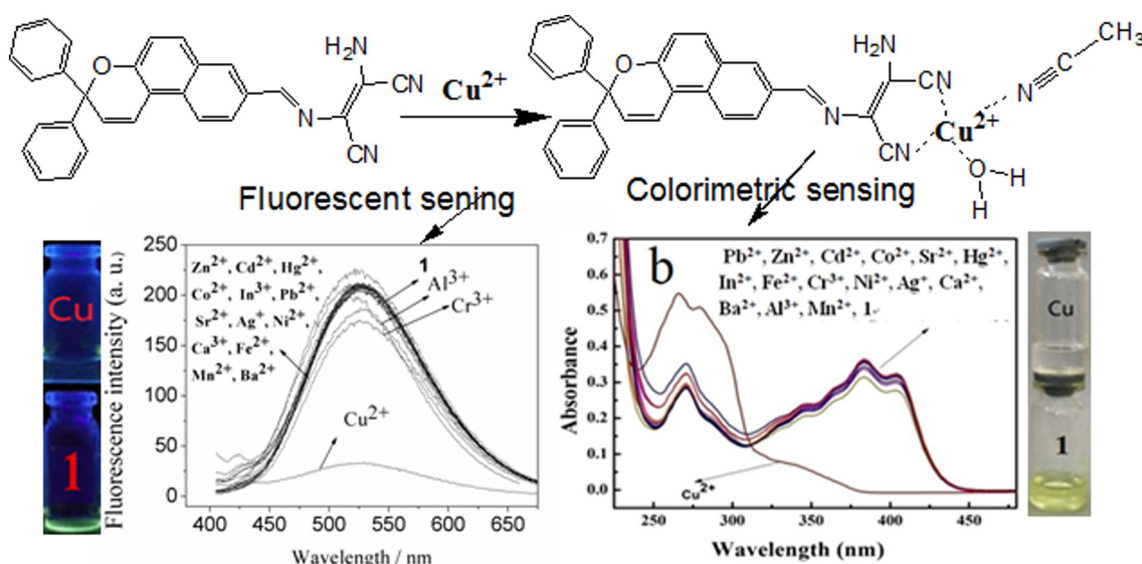


Fig. 11. Optimized ground-state geometries and frontier orbital shapes of free sensor **1** and sensor **1** + Cu^{2+} complex. Color code: C (gray), N (blue), H (white), O (red), Cu (orange). (For interpretation of the references to color in this figure legend, the reader is referred to the web version of this article.)



Scheme 2. The complex mode and sensing mechanism of sensor **1** towards Cu^{2+} ion.

from HOMO, the lowest unoccupied orbit (LUMO) was mainly located on the naphthalene unit and diaminomaleonitrile moiety. Their band gap between HOMO (-5.55 eV) and LUMO (-2.45 eV) was calculated as 3.08 eV. When copper ion coordinated with the diaminomaleonitrile moiety, obvious changes had taken place in the orbital distribution and band gaps. The change of α -HOMO of complex was very little, however, the β -HOMO remarkably focus on the benzene ring from pyran and naphthalene units. Compared with LUMO of free sensor **1**, α -LUMO of complex was mainly situated on naphthopyran and diaminomaleonitrile units and hardly on the benzene rings. β -LUMO was also mainly on the naphthopyran unit and few on the benzene rings. The band gaps both α orbits (2.82 eV) and β (1.29 eV) orbits reduced significantly compared with that of free sensor **1** (3.08 eV), which indicated the complex was more stable. Generally, a molecule with low HOMO energy level will be more stable and consequently more un-reactive. In this case, all the α orbits and β orbits energy levels of complex were more lower than those of free sensor **1**, respectively, which further confirmed higher stability of sensor **1** + Cu^{2+} complexes. The above DFT results had further explained the formation of sensor **1** + Cu^{2+} complexes with 1:1 stoichiometry.

Based on all the results of Job's plot, mass spectra and Benesi-Hildebrand plot, ^1H NMR titration and theoretical calculation, it was confirmed the selective colorimetric and fluorescent responses of sensor **1** towards Cu^{2+} ions could be ascribed to the selective coordination of sensor **1** with Cu^{2+} via the two nitrogen atoms of $-\text{C}\equiv\text{N}$ on the diaminomaleonitrile unit. The complex mode and sensing mechanism of sensor **1** towards Cu^{2+} ion was illustrated in Scheme 2.

4. Conclusions

In this paper, a naphthopyran-diaminomaleonitrile dyad (sensor **1**) as multifunctional materials was designed and prepared. Sensor **1** displayed excellent photochromic property and photochromic fluorescence switch performance with well fatigue resistance. The fluorescence intensity of sensor **1** can be modulated reversibly via the alternative UV irradiation and put in the dark. Sensor also **1** displayed the high selective absorbance and fluorescence response towards Cu^{2+} ions accompanied by the obvious color change from yellow to colorless. In addition, both the absorbance and fluorescence intensities presented good linear relationship with the Cu^{2+} concentration. Sensor **1** can be used as colorimetric and fluorescent sensing for Cu^{2+} ion to monitor Cu^{2+} ion in water. The results of Job's plot, mass spectra, ^1H NMR titration and quantum calculation demonstrated that the sensing

mechanism was the complex formation of sensor **1** with Cu^{2+} ion with 1:1 stoichiometry, in which, the diaminomaleonitrile was the coordination unit. Sensor **1** displayed great potential to be used as photochromic material, colorimetric and fluorescent sensor for Cu^{2+} ions, so we hope these results will promote the rational design of more excellent functional materials in the future.

CRediT authorship contribution statement

Heyang Zhang: Investigation. **Tianyuan Zhong:** Investigation, Formal analysis. **Nan Jiang:** Formal analysis. **Zhuo Zhang:** Investigation. **Xue Gong:** Investigation. **Guang Wang:** Methodology, Writing - original draft.

Declaration of competing interest

The authors confirm that this manuscript has been read and approved by all named authors, there are no known conflicts of interest associated with this publication and there has been no significant financial support for this work that could have influenced its outcome.

Acknowledgement

This work was supported by the National Natural Science Foundation of China (no. 50873019) and Research Fund for the Doctoral Program of Higher Education of China (20120043110007).

Appendix A. Supplementary data

Supplementary data to this article can be found online at <https://doi.org/10.1016/j.saa.2020.118191>.

References

- [1] A. Fihey, A. Perrier, W.R. Browne, D. Jacquemin, Multiphotochromic molecular systems, *Chem. Soc. Rev.* 44 (2015) 3719–3759.
- [2] H. Tian, S. Wang, Photochromic bisthiénylene as multi-function switches, *Chem. Commun.* (2007) 781–792.
- [3] L. Liu, X. Xie, D. Jia, J. Guo, X. Xie, Synthesis and properties of a novel photochromic compound with modulated fluorescence in the solid state, *J. Org. Chem.* 75 (2010) 4742–4747.
- [4] L. Liu, A. Wang, G. Wang, J. Li, Y. Zhou, A naphthopyran-rhodamine based fluorescent and colorimetric chemosensor for recognition of common trivalent metal ions and Cu^{2+} ions, *Sensors Actuators B Chem.* 215 (2015) 388–395.
- [5] D. Li, J. Jiang, Q. Huang, G. Wang, M. Zhang, J. Du, Light-triggered “on-off” switching of fluorescence based on a naphthopyran-containing compound polymer micelle, *Polym. Chem.* 7 (2016) 3444–3450.

- [6] Y. Zhang, Y. Zhang, G. Wang, Y. He, Study on fluorescent switching of naphthopyran and pyrene-containing dyad and copolymer in solutions and films, *Dyes Pigments* 102 (2014) 107–113.
- [7] M. Zhang, D. Li, G. Wang, J. Li, H. Sun, Highly efficient light-induced reversible micellization of amphiphilic polymer based on photochromism of naphthopyran in aqueous solution, *Dyes Pigments* 105 (2014) 232–237.
- [8] L. He, B. Dong, Y. Liu, W. Lin, Fluorescent chemosensors manipulated by dual/triple interplaying sensing mechanisms, *Chem. Soc. Rev.* 45 (2016) 6449–6461.
- [9] S.L. Wang, C. Li, Q.H. Song, Fluorescent chemosensor for dual-channel discrimination between phosgene and triphosgene, *Anal. Chem.* 91 (2019) 5690–5697.
- [10] P. Su, Z. Zhu, J. Wang, B. Cheng, W. Wu, K. Iqbal, Y. Tang, A biomolecule-based fluorescence chemosensor for sequential detection of Ag^+ and H_2S in 100% aqueous solution and living cells, *Sensors Actuators B Chem.* 273 (2018) 93–100.
- [11] L. Mao, Y. Liu, S. Yang, Y. Li, X. Zhang, Y. Wei, Recent advances and progress of fluorescent bio-/chemosensors based on aggregation-induced emission molecules, *Dyes Pigments* 162 (2019) 611–623.
- [12] M.C. Linder, M. Hazegh-Azam, Copper biochemistry and molecular biology, *Am. J. Clin. Nutr.* 63 (1996) 797S–811S.
- [13] K.S. Mani, R. Rajamanikandan, B. Murugesapandian, R. Shankar, G. Sivaraman, M. Llanchehan, S.P. Rajendran, Coumarin based hydrazone as an ICT-based fluorescence chemosensor for the detection of Cu^{2+} ions and the application in HeLa cells, *Spectrochim. Acta A Mol. Biomol. Spectrosc.* 214 (2019) 170–176.
- [14] D. Liu, W. Chen, K. Sun, K. Deng, W. Zhang, Z. Wang, X. Jiang, Resettable, multi-readout logic gates based on controllably reversible aggregation of gold nanoparticles, *Angew Chem Int Ed Engl* 50 (2011) 4103–4107.
- [15] R. Uauy, M. Olivares, M. Gonzalez, Essentiality of copper in humans, *Am. J. Clin. Nutr.* 67 (1998) 952S–959S.
- [16] Y.F. Tan, N. O'Toole, N.L. Taylor, A.H. Millar, Divalent metal ions in plant mitochondria and their role in interactions with proteins and oxidative stress-induced damage to respiratory function, *Plant Physiol.* 152 (2010) 747–761.
- [17] V. Desai, S.G. Kaler, Role of copper in human neurological disorders, *Am. J. Clin. Nutr.* 88 (2008) 855S–858S.
- [18] H. Shoaee, M. Roshdi, N. Khanlarzadeh, A. Beiraghi, Simultaneous preconcentration of copper and mercury in water samples by cloud point extraction and their determination by inductively coupled plasma atomic emission spectrometry, *Spectrochim. Acta A Mol. Biomol. Spectrosc.* 98 (2012) 70–75.
- [19] G. Özyeybek, S. Erarpat, D.S. Chormey, M. Firat, Ç. Büyükpınar, F. Turak, S. Bakirdere, Sensitive determination of copper in water samples using dispersive liquid-liquid microextraction-slotted quartz tube-flame atomic absorption spectrometry, *Microchem. J.* 132 (2017) 406–410.
- [20] J. Giersz, M. Bartosiak, K. Jankowski, Sensitive determination of Hg together with Mn, Fe, Cu by combined photochemical vapor generation and pneumatic nebulization in the programmable temperature spray chamber and inductively coupled plasma optical emission spectrometry, *Talanta* 167 (2017) 279–285.
- [21] D. Grujicic, B. Pesic, Electrodeposition of copper: the nucleation mechanisms, *Electrochim. Acta* 47 (2002) 2901–2291.
- [22] L. Wang, Q. Bing, J. Li, G. Wang, A new “ON-OFF” fluorescent and colorimetric chemosensor based on 1,3,4-oxadiazole derivative for the detection of Cu^{2+} ions, *J. Photochem. Photobiol. A Chem.* 360 (2018) 86–94.
- [23] Q. Bing, L. Wang, D. Li, G. Wang, A new high selective and sensitive turn-on fluorescent and ratiometric absorption chemosensor for Cu^{2+} based on benzimidazole in aqueous solution and its application in live cell, *Spectrochim. Acta A Mol. Biomol. Spectrosc.* 202 (2018) 305–313.
- [24] L. Wang, X. Gong, Q. Bing, G. Wang, A new oxadiazole-based dual-mode chemosensor: colorimetric detection of Co^{2+} and fluorometric detection of Cu^{2+} with high selectivity and sensitivity, *Microchem. J.* 142 (2018) 279–287.
- [25] S.M.S.R. Ali, I.A.I. Ali, A novel, highly sensitive, selective, reversible and turn-on chemi-sensor based on schiff base for rapid detection of Cu (II), *Spectrochim. Acta Part A: Mol. Biomol. Spectrosc.* 183 (2017) 225–231.
- [26] Z. Chen, L. Wang, G. Zou, et al., Highly selective fluorescence turn-on chemosensor based on naphthalimide derivatives for detection of copper (II) ions, *Spectrochim. Acta A Mol. Biomol. Spectrosc.* 105 (2013) 57–61.
- [27] Z.Y. Gündüz, C. Gündüz, C. Özpınar, O.A. Uruçu, A novel Schiff-base as a Cu (II) ion fluorescent sensor in aqueous solution, *Spectrochim. Acta A Mol. Biomol. Spectrosc.* 136 (2015) 1679–1683.
- [28] R. Vikneswaran, M.S. Syafiq, N.E. Eltayeb, M.N. Kamaruddin, S. Ramesh, R. Yahya, A new thio-Schiff base fluorophore with copper ion sensing, DNA binding and nuclease activity, *Spectrochim. Acta A Mol. Biomol. Spectrosc.* 150 (2015) 175–180.
- [29] J. Yin, Q. Bing, L. Wang, G. Wang, Ultrasensitive and highly selective detection of Cu^{2+} ions based on a new carbazole-Schiff, *Spectrochim. Acta A Mol. Biomol. Spectrosc.* 189 (2018) 495–501.
- [30] Y. Zhao, G. Wang, J. Zhang, Study on fluorescent switching of naphthopyran with carbazole and pyrene dyad immobilized on SBA-15, *Tetrahedron* 70 (2014) 5966–5973.
- [31] M.-D. Zhang, Y.-F. Zhang, D.-H. Li, G. Wang, J.-X. Li, The high stability of merocyanine and significant slow fading speed of naphthopyran in layer-by-layer assembled films via hydrogen bonding, *New J. Chem.* 37 (2013) 1385.
- [32] R.F. Khairutdinov, K. Giertz, J.K. Hurst, E.N. Voloshina, N.A. Voloshin, V.I. Minkin, Photochromism of spirooxazines in homogeneous solution and phospholipid liposomes, *J. Am. Chem. Soc.* 120 (1998) 12707–12713.
- [33] X. Zhang, G. Wang, K. Zhang, Photochromic behavior of naphthopyran in styrene-butadiene-styrene elastomer thin films: effect of stretching of film and linker, *J. Appl. Polym. Sci.* 127 (2013) 1794–1802.
- [34] D. Li, A. Munyentwali, G. Wang, M. Zhang, S. Xing, Light and temperature responsive block copolymer assemblies with tunable fluorescence emissions, *Dyes Pigments* 117 (2015) 92–99.
- [35] Y. He, J. Yin, G. Wang, New selective “on-off” fluorescence chemosensor based on carbazole Schiff base for Fe^{3+} detection, *Chem. Heterocycl. Compd.* 54 (2018) 146–152.
- [36] M. Strianese, C. Pellicchia, Metal complexes as fluorescent probes for sensing biologically relevant gas molecules, *Coord. Chem. Rev.* 318 (2016) 16–28.
- [37] S. Mirra, S. Milione, M. Strianese, C. Pellicchia, A copper porphyrin for sensing H_2S in aqueous solution via a “coordinative-based” approach, *Eur. J. Inorg. Chem.* 2015 (2015) 2272–2276.
- [38] J. Liu, Y. Lu, A DNAzyme catalytic beacon sensor for paramagnetic Cu^{2+} ions in aqueous solution with high sensitivity and selectivity, *J. Am. Chem. Soc.* 129 (2007) 9838–9839.
- [39] H.S. Jung, P.S. Kwon, J.W. Lee, J.I. Kim, C.S. Hong, J.W. Kim, S.H. Yan, J.Y. Lee, J.H. Lee, T. Joo, J.S. Kim, Coumarin-derived Cu^{2+} selective fluorescence sensor: synthesis, mechanisms, and applications in living cells, *J. Am. Chem. Soc.* 131 (2009) 2008–2012.
- [40] M.J. Frisch, G.W. Trucks, H.B. Schlegel, G.E. Scuseria, M.A. Robb, J.R. Cheeseman, G. Scalmani, V. Barone, B. Mennucci, G.A. Petersson, H. Nakatsuji, M. Caricato, X. Li, H.P. Hratchian, A.F. Maylov, J. Bloino, G. Zheng, J.L. Sonnenberg, M. Hada, M. Ehara, K. Toyota, R. Fukuda, J. Hasegawa, M. Ishida, T. Nakajima, Y. Honda, O. Kitao, H. Nakai, T. Vreven, J.A. Montgomery, J.E. Peralta, F. Gliaro, M. Bearpark, J.J. Heyd, E. Brothers, K.N. Kudin, V.N. Staroverov, R. Kobayashi, J. Normand, K. Raghavachari, A. Rendell, J.C. Burant, S.S. Iyengar, J. Tomasi, M. Cossi, N. Rega, J.M. Millam, M. Klene, J.E. Knox, J.B. Cross, V. Bakken, C. Adamo, J. Jaramillo, R. Gomperts, R.E. Stratmann, O. Yazyev, A.J. Austin, R. Cammi, C. Pomelli, J.W. Ochterski, R.L. Martin, K. Morokuma, V.G. Zakrzewski, G.A. Voth, P. Salvador, J.J. Dannenberg, S. Dapprich, A.D. Daniels, Ö. Farkas, J.B. Foresman, J.V. Ortiz, J. Cioslowski, D.J. Fox, Gaussian 09, Revision B.01, Gaussian, Inc, Wallingford, CT, 2009.
- [41] C.Y. Legault, CYL view, 1.0b, Université de Sherbrooke, Sherbrooke, Quebec, Canada, 2009.
- [42] A.D. Becke, Density-functional thermochemistry. III. The role of exact exchange, *J. Chem. Phys.* 98 (1993) 5648–5652.
- [43] W.R. Wadt, P.J. Hay, Ab initio effective core potentials for molecular calculations. Potentials for main group elements Na to Bi, *J. Chem. Phys.* 82 (1985) 284–298.
- [44] P.J. Hay, W.R. Wadt, Ab initio effective core potentials for molecular calculations. Potentials for K to Au including the outermost core orbitals, *J. Chem. Phys.* 82 (1985) 299–310.
- [45] J. Andzelm, S. Huzinaga, Gaussian Basis Sets for Molecular Calculations, Elsevier Science, New York, 1984.